




RESEARCH ARTICLE

RapidBenthos: Automated segmentation and multi-view classification of coral reef communities from photogrammetric reconstruction

Tiny Remmers^{1,2}  | Nader Boutros³ | Mathew Wyatt³  | Sophie Gordon² | Maren Toor² | Chris Roelfsema⁴ | Katharina Fabricius² | Alana Grech¹  | Marine Lechene^{1,2} | Renata Ferrari²

¹College of Science and Engineering, James Cook University, Townsville, Queensland, Australia

²Australian Institute of Marine Science, Cape Cleveland, Queensland, Australia

³Australian Institute of Marine Science, Crawley, Western Australia, Australia

⁴School of the Environment, University of Queensland, Brisbane, Queensland, Australia

Correspondence

Tiny Remmers

Email: tiny.remmersbarry@my.jcu.edu.au

Funding information

Australian Government's Reef Trust; Great Barrier Reef Foundation; Australian Institute of Marine Science; College of Science and Engineering at James Cook University; Remote Sensing Research Centre of the School of the Environment at the University of Queensland

Handling Editor: Chloe Robinson

Abstract

1. Underwater photogrammetry is routinely used to monitor large areas of complex and heterogeneous ecosystems, such as coral reefs. However, deriving data on benthic components (i.e. sand, rubble, coral and algae) from photogrammetry products has remained challenging due to the highly time-consuming process of manual data extraction.
2. We developed a machine learning approach to quantify benthic community composition in coral reefs from orthomosaics, which requires no manual delineation of benthic components for training or implementation. The current study presents RapidBenthos, an automated workflow that segments and classifies large-area images. Our pipeline (1) uses a pre-trained segmentation model, eliminating the need for manually generated fine-scale segmented training data, and (2) classifies the resulting segments from multiple views using the underlying survey images, allowing for classification to fine taxonomic levels.
3. Within a test photomosaic built from a coral reef area of 40 m⁻², the model automatically detected 43 different benthic classes. Validation resulted in an overall classification accuracy of 0.96 and a segmentation accuracy of 0.87, when compared to a manually digitised replica. The RapidBenthos workflow was 195 times faster than manual segmentation and classification. Additional validation of 524 *Acropora* coral colonies from 11 additional test plots resulted in a segmentation accuracy of 0.92 and classification accuracy of 0.88 to the coarser 'Acropora' group.
4. RapidBenthos has the capability to extract an unprecedented level of data from photomosaics of coral reefs or other complex environments, allowing to sustainably scale photogrammetric monitoring technique both in replicate and survey extent, which consequently can lead to new research questions and more informed ecosystem management.

This is an open access article under the terms of the [Creative Commons Attribution-NonCommercial-NoDerivs](https://creativecommons.org/licenses/by-nc-nd/4.0/) License, which permits use and distribution in any medium, provided the original work is properly cited, the use is non-commercial and no modifications or adaptations are made.

© 2024 The Author(s). *Methods in Ecology and Evolution* published by John Wiley & Sons Ltd on behalf of British Ecological Society.

KEYWORDS

artificial intelligence, automatic segmentation, benthic community composition, coral reefs, machine learning, photogrammetry, ReefCloud point annotation, Segment Anything Model

1 | INTRODUCTION

Community composition is the type and relative abundances of taxa present in a sample (Bowker et al., 2021). It quantifies metrics describing the spatial organisation and entropy of ecosystem constituents (Loke & Chisholm, 2022) and is fundamental to assess ecosystem status and condition. In-situ time-series data on community composition allow for tracking changes in ecosystem condition and resilience (Vercelloni et al., 2024), providing valuable insights for management. For example, understanding shifts in community composition following a disturbance can inform spatial prioritisation for interventions, leading to more effective management or restoration (Bellwood et al., 2019; Boström-Einarsson et al., 2020; Evans et al., 2015; Nolan et al., 2021). However, for coral reefs, assessing changes over time is challenging due to the high heterogeneity and complexity of reef communities, the varying scales of study (from centimetres to thousands of kilometres), the remoteness of some marine environments and difficulties in underwater data collection (Hamylton, 2017; Madin et al., 2016; Obura et al., 2019).

Over the past decade, the adoption of close-range underwater photogrammetry (hereafter referred to as photogrammetry) in coral reef studies has grown significantly, becoming a standard method for monitoring these ecosystems (Bayley et al., 2019; Figueira et al., 2015; Miller et al., 2021; Nocerino et al., 2020; Obura et al., 2019; Remmers et al., 2023; Urbina-Barreto, Garnier, et al., 2021). Photogrammetry is the science of measuring and interpreting objects from images, typically by combining individual images into 3D reconstructions of large seafloor areas (tens to thousands square metres). This technique allows for continuous observation of the seafloor while preserving the spatial distribution of benthic features (Aber et al., 2010; Figueira et al., 2015; Luhmann, 2011). Orthomosaics, the two dimensional projections of these reconstructions, enable the derivation of community-level metrics, such as colony size frequency distribution, clustering, density and traditional habitat metrics such as percentage cover of benthic classes (Ferrari et al., 2021; Hopkinson et al., 2020; Marre et al., 2019; Miller et al., 2021; Urbina-Barreto, Chiroleu, et al., 2021). This ecological information is essential to build robust indicators of ecosystem status and trends, informing scientists, practitioners and decision-makers in coral reefs management (Bellwood et al., 2019; Boström-Einarsson et al., 2020; Evans et al., 2015; Ferrari et al., 2021; Nolan et al., 2021).

A key challenge in using photogrammetry for coral reef studies is the limited capacity to efficiently quantify community composition and extract colony-level metrics from orthomosaics (Bellwood et al., 2019; Johnson-Roberson et al., 2006; Remmers et al., 2023; Rossi et al., 2021; Shihavuddin et al., 2013). Two common methods to quantify community composition at the scale of individual reef

images are: (1) point classification, where several points are randomly or systematically placed and labelled (Beijbom et al., 2012; Kohler & Gill, 2006), and (2) segmentation, where similar pixels are grouped to delineate object contours (Pavoni et al., 2020). Currently, few techniques can apply these methods to orthomosaics, which cover much larger reef areas than individual photographs and can be scaled using ground control points (GCPs) of known position (Lechene et al., 2019). Classifying and segmenting orthomosaics would greatly increase our ability to quantify coral colony size, community composition, per cent cover, taxa distribution and mortality (Ferrari et al., 2021; Hopkinson et al., 2020; Marre et al., 2019; Miller et al., 2021; Urbina-Barreto, Chiroleu, et al., 2021).

Although few studies (Mills et al., 2023; Schürholz & Chennu, 2022) have successfully achieved high-thematic detail classification of underwater images using hyperspectral imagery, hyperspectral cameras remain significantly more expensive and require advanced user training, posing logistical constraints for their routine deployment in monitoring programmes. A recent review on photogrammetry in coral reef ecology revealed that less than 45% of studies used benthic annotation methods to quantify communities, missing valuable data (Remmers et al., 2023). Notably, only five out of 55 studies used automatic orthomosaic segmentation, all limited to eight classes (Remmers et al., 2023). This gap is due to the substantial human effort required for manual segmentation—about 1 h per square metre (Pavoni et al., 2020). Furthermore, automating segmentation with deep learning faces challenges due to the high complexity, heterogeneity, and diversity of constituents and reef habitats, and the large amount of training data required to represent them (Beijbom et al., 2012; González-Rivero et al., 2020; Li et al., 2024; Pavoni et al., 2020; Yuval et al., 2021).

A terrestrial case study on urban street scenes (called 'CityScape'), featuring 30 classes grouped into eight categories, required the manual input of 5000 densely segmented images and 20,000 weakly annotated images totalling over 9833 h of manual labour before deep learning model training (Cordts et al., 2016). Given the lower complexity and heterogeneity of urban images—characterised by contrasting colours, well-defined edges, straight lines and right angles—compared with coral reefs, this underscores the substantial manual effort needed to apply such techniques to this more complex environment. Thus, there is a strong need for rapid, automated and repeatable technique to segment, classify and extract community composition data from underwater orthomosaics to fully leverage the benefits of photogrammetry.

Widespread development of artificial intelligence (AI) has enabled its integration into monitoring tools. One such tool, ReefCloud, utilises a machine learning (ML) model trained on coral reef benthic images collected by the Australian Institute of Marine Science (AIMS) Long-Term Monitoring Program (LTMP), which consists of

millions of image points classified by professional benthic ecologists. ReefCloud requires users to label a subset of their uploaded images to fine-tune the model to the specifics of their dataset and provide accurate label predictions. This approach allows automated estimates of coral reef benthic composition to be generated up to 700 times faster than manual assessment (González-Rivero et al., 2020; ReefCloud, 2022).

Recently released foundational models have shown improved performance on novel datasets, such as underwater images, even when applied with little or no in-domain training data. The Segment Anything Model (SAM) is a highly generalisable segmentation model, which can comprehend and make predictions about unfamiliar objects or concepts (e.g. seafloor orthomosaics) not encountered during its training phase (Kirillov et al., 2023).

We introduce 'RapidBenthos', a workflow for automated semantic segmentation and classification of large-extent orthomosaics (40–72 m²). Our workflow utilises the pre-trained SAM (Kirillov et al., 2023) in conjunction with the online ReefCloud point classification tool (ReefCloud, 2022) to eliminate the need for manually segmented training data. We describe the RapidBenthos methodology, including segmentation, classification and quantification of community composition from orthomosaics. Subsequently, the model is validated using performance metrics (e.g. Intersection over Union [IoU], F1 score, accuracy). Finally, the results, advantages and limitations of the method are discussed.

2 | METHOD

2.1 | Data acquisition

Data for the primary validation of the RapidBenthos workflow were collected on an exposed reef slope off Lizard Island (14.69°S, 145.46°E) in the northern offshore Great Barrier Reef (GBR) in October 2021 (Figure 1a). The site had an average depth of five metres, covered an area of 72 sq. m and featured diverse benthic components, composed of a mix of hard and soft coral, algae and abiotic substrate elements such as sand and rubble. The site was selected for primary validation due to its diverse benthic composition and moderate coral cover (~20%), which rendered it suitable for complete (100% of area) manual segmentation and classification. To evaluate RapidBenthos across various environmental conditions and reef habitats, the most common class, *Acropora corymbose*, was validated against manually segmented colonies at an additional 11 sites (72 sq. m) across the GBR and Torres Strait (see Supporting Information S1 for details). This work was conducted under the Great Barrier Reef Marine Park permit G21/44774.1.

All sites were imaged using a standardised diver-rig photogrammetry workflow described by Gordon et al. (2023). High-resolution benthic images (5686 × 3217 pixels) were captured using two Nikon D850 DSLR cameras with 20mm Nikkor prime lens shooting at 0.5 s intervals (full camera settings described in Gordon et al., 2023).

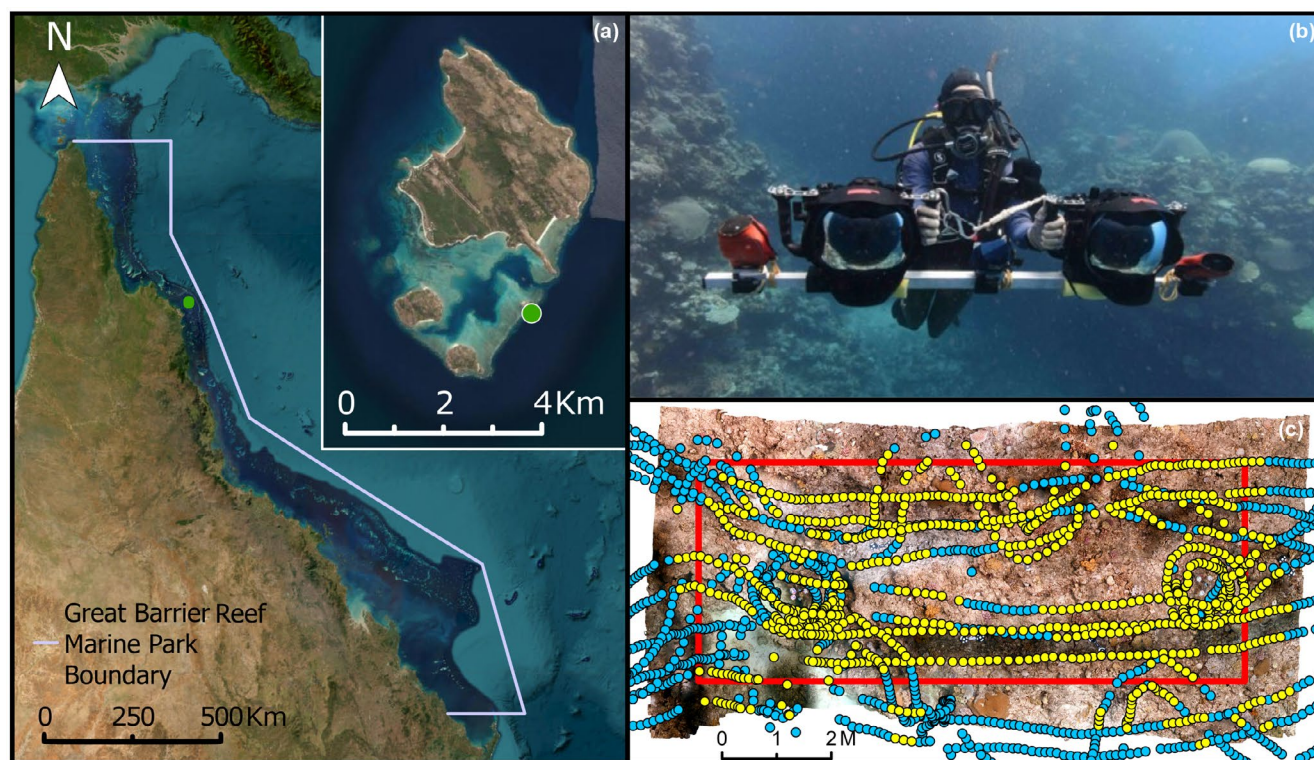


FIGURE 1 Study location and site imaging techniques. (a) Lizard Island showing the primary validation site on the wave-exposed eastern side (green dot); (b) SCUBA diver with DSLR photogrammetry camera rig; and (c) photogrammetry imaging pattern showing camera location (blue and yellow dots), images used for analyses (yellow dots) and data analysis extent (red line).

Cameras were housed in Nauticam underwater housings with 8.5-inch dome ports and were mounted on an aluminium rig at a distance of 57 cm between lenses (Figure 1b). Around 3000 nadir and oblique photographs were captured per site at an altitude of approximately 1.5 m (80% overlap between adjacent images) using a 'lawn-mowing' swim pattern consisting of five longitudinal passes and an additional four to eight perpendicular passes (Figure 1c). Six GCPs were distributed across the depth gradient of the site prior to imaging to scale and orient resultant models in X, Y and Z axes (details provided in Gordon et al., 2023). Depth was also recorded for each GCP to incorporate bathymetric information into 3D model building.

2.2 | Building 2D and 3D models

All models were constructed using Agisoft Metashape Professional v1.7.6 (Agisoft LLC, St. Petersburg, Russia) using a photogrammetry processing protocol described in Appendix S1. Images were automatically filtered using the 'Image Quality' parameter in Metashape (quality threshold of 0.5) prior to running initial low-quality alignment. GCP markers were then detected, and depth information imported to scale models before re-aligning points at high quality. Resultant high-quality sparse point clouds were then filtered, and cameras optimised to reduce model reprojection error. High-quality depth maps were then generated from the filtered high-quality sparse point clouds and used to generate textured meshes. Textured meshes were cropped to the 72 sq. m area of interest and high pixel resolution ($\sim 0.353 \text{ mm}^2$) orthomosaics were generated. To ensure even coverage for the primary validation plot, the distorted edge was removed by cropping the orthomosaic to an area of 40 sq. m for RapidBenthos analysis and validation.

2.3 | Point classification model training

The online platform ReefCloud was used to classify the photogrammetry imagery collected in the current study (ReefCloud, 2022). A total of 1700 images were selected from photogrammetry imagery of multiple sites around Lizard Island to train the point annotation model used for primary validation. Images were selected to ensure that the model was trained on images encompassing the diversity of benthic components present. A total of 33,937 points were manually classified, with 80% used to train the classification model and the remaining 20% reserved for testing the model's performance.

The label set used for point classification consisted of 73 classes and followed a hierarchical design (functional group < coarse class < genus < species), to ensure that every benthic component could be labelled. The coarse-class categories were selected following the Collaborative and Automated Tools for Analysis of Marine Imagery (CATAMI) classification scheme (Althaus et al., 2015) and included: *Acropora*, branching non-*Acropora*, massive coral, foliose, encrusting, columnar, *Fungiidae*, fire coral, anemone, *Zoanthid*, soft coral,

sponge, algae, abiotic substrate, mobile biota, water, markers and unidentifiable (Appendix S2).

2.4 | RapidBenthos workflow

The RapidBenthos pipeline is a two-stage process to segment and classify large-area orthomosaics of coral reefs, which utilises: (1) a pre-trained, open-source ML segmentation model (SAM) to segment the orthomosaic and (2) a point classification model (ReefCloud) to classify the resulting segments from multiple views using the high-resolution images underlying the orthomosaics (Figure 2; Appendix S3). The computational processing conducted in this study used Python 3.9.16 on a High-Performance Computing (HPC) with a NVIDIA A100 PCIe 40GB GPU node. All processing steps are run on Python IDE, a quick start processing steps is described in Appendix S4.

2.5 | Orthomosaic segmentation

Orthomosaics were segmented using the SAM-geospatial repository (Wu & Osco, 2023) with two different sliding windows dimensions and number of sampling points per window (4600 pixels with 128 sample points per side and 8400 pixels with 200 sample points per side) (Figure 2a; Appendix S3). Processing the segmentation twice with varying sliding window dimensions assured window edge overlap and resulted in fully closed geometries. We tested various combinations of window sizes and sampling points per side, concluding that larger windows more reliably detected larger objects, while higher sampling points yielded more precise segmentation. As larger windows and more sampling points increased computing time, the chosen values represent an optimal balance between segmentation accuracy and computational efficiency.

The two resulting rasters were combined using Gdal raster calculator, and the output was transformed to a polygon layer using the `tiff_to_gpkg` function. The `Filter_segment` function was applied to lower the number of segments within colony boundaries, remove background polygons ($\text{area} \geq 2.5 \text{ m}^2$), and polygons smaller than 0.00005 m^2 (Appendix S3). The resulting segments and corresponding centre points were exported as shapefiles (Figure 2b).

2.6 | Orthomosaic classification

Labelling of segments was attributed from point classification of underlying photographs used for orthomosaic generation. Applying the `camera_point_from_segment_centerPoint` function in the python IDE, the 3D vertices corresponding to each segment's centre point were extracted from the 3D mesh (Figure 2c; Appendix S3). Next, all photographs capturing each vertex were selected based on two conditions: (1) the camera was enabled in the Metashape Pro project; (2) the pixel capturing the vertex was in the 40% central

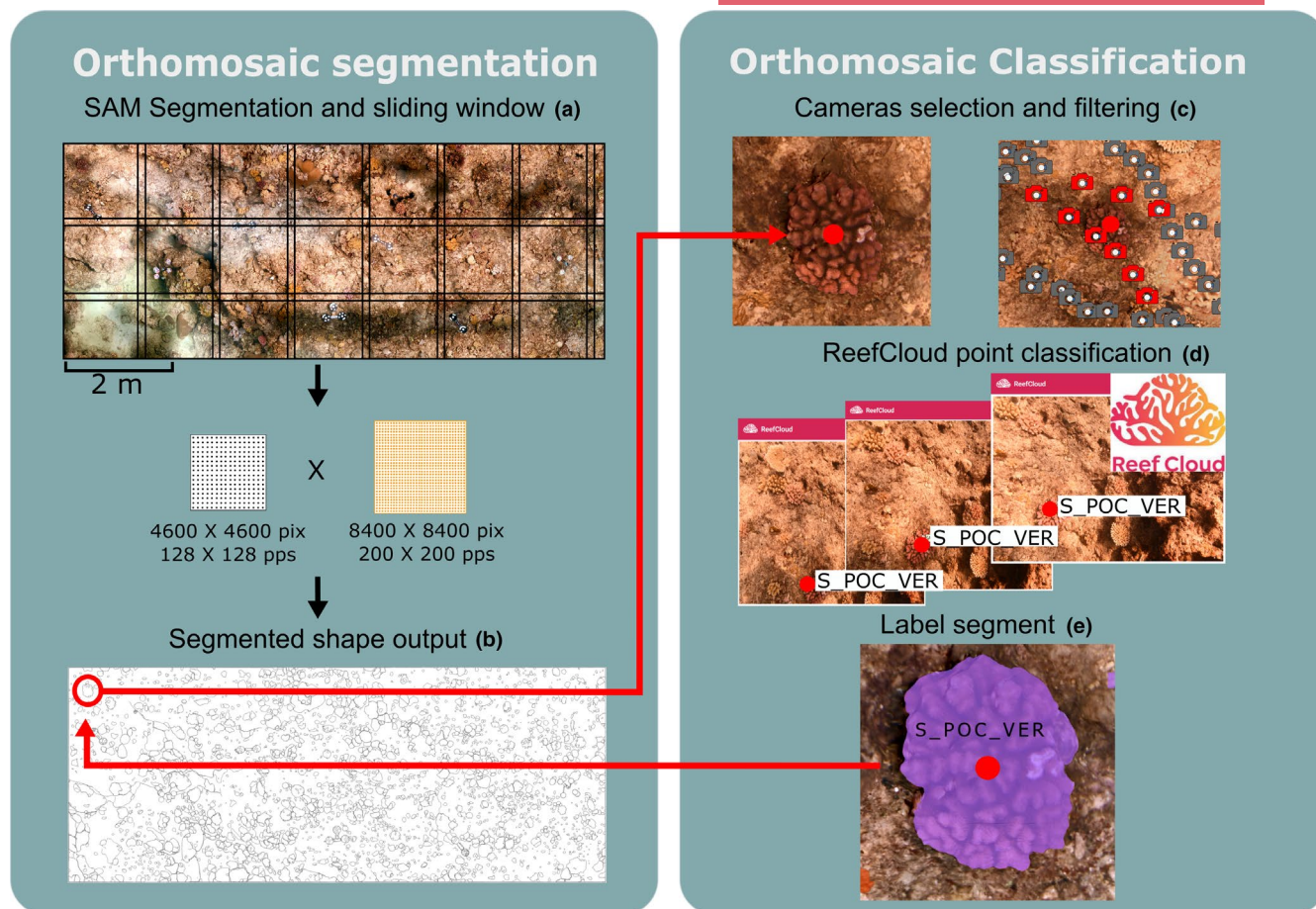


FIGURE 2 Workflow schematic describing the two-step process of orthomosaic segmentation followed by segment classification. (a) The segmentation first applies Segment Anything Model (SAM) using two different sliding windows (i.e. 4600 pix with 128 sampling points and 8400 pix with 200 sampling points) resulting in closed geometries due to windows' edge overlap and subsequently; (b) converts the output to shapes; (c) the annotation then iterates through all segments to find the 10 best photographs (red cameras icons) capturing the segments' centre point (red circle) then; (d) classifies the points on the photographs using ReefCloud and finally; (e) assigns the best label to the segment.

region of the image (not within a 750-pixel margin of all edges of the photograph). These thresholds aimed, respectively, at removing low-quality images and classification points located near distorted edges of the images.

To reduce computation time, for each segment the 10 closest photographs to the centre point of the segment, based on the 2D distance between the camera centre and vertex in the 3D mesh, were selected (Figure 2d). Once the 10 images were selected for a segment, a single point per image was classified using ReefCloud. To attribute a class to a segment, we first used the ReefCloud model to assign each point within the selected 10 photographs a label and a prediction score (representing an estimate of prediction probability), which resulted in 10 labels per segment. All labels for each segment were then filtered by the most common coarse class and a prediction score higher than 0.4. The final label was selected using Equation (1), and the final classes were then assigned to their respective segments by selecting the class with the maximum weighted prediction score (Figure 2e).

$$\text{MAX_wPred} = N \times \text{mPred_score}. \quad (1)$$

Example for segment A

- $\text{MAX_wPred_S_POC_VER} = (8 \times 0.85) = 6.8$
- $\text{MAX_wPred_S_POC_DAM} = (2 \times 0.6) = 1.2$
- Therefore, class = S_POC_VER

where MAX_wPred is the maximum weighted prediction score, N is the number of occurrences of a given class, and mPred_score is the mean prediction score.

2.7 | Per cent cover of the benthic components

To obtain a fully annotated orthomosaic and determine site community composition as per cent cover of the different benthic components, including abiotic and algae cover without distinctive edges, the areas between classified segments were annotated using a hexagonal grid (hexagrid) of 0.0025 m^2 cells. A hexagrid was selected over a regular square grid as it ensures equal distances to the centroid for each

neighbouring point, thereby providing a better representation of the area surrounding each point. The hexagrid was then clipped to remove any overlapping area with the segmented layer, and the centre point for all remaining cells were exported as CSV file. Point classification protocols described in Sections 2.3 and 2.4, Figure 2 and Appendix S3 were then employed. Once the hexagrid was classified, the layer was merged with the segmented layer and the per cent cover for all classes was determined by computing the proportion of the surface covered by each class relative to the total extent of the orthomosaic.

2.8 | Colony-level metrics

Running SAM twice during the segmentation phase of RapidBenthos can lead to single colonies composed of more than one segment (Section 2.5). To address this artefact and obtain colony-level metrics such as colony count and planar area, segments belonging to the same colony can be merged. All segments were first filtered by class and all adjacent segments of the same class were merged except for the classes included in the coarse classes 'Acropora', 'branching non-Acropora' and 'soft coral'. Since these remaining classes can have neighbouring colonies of the same class, the remaining segments were merged based on a size threshold smaller than 0.0025 m² (6.2 cm diameter), to minimise the probability of merging adjacent colonies. Only segments smaller than the threshold were merged to neighbouring segments of the same class.

2.9 | Validation data

Validation data were created using TagLab V.2023.3.16 9 (Pavoni et al., 2021). All visible benthic components were segmented and classified to the finest taxonomic resolution possible. A total of 60 h of manual input was necessary to segment and classify 1027 benthic components from the 72 m² orthomosaic (approximately 17 segments per hour). To ensure the accuracy of orthomosaic annotations, the manually segmented and classified orthomosaic was quality checked by an additional independent annotator. This quality checked process took an additional 5 h of manual input and resulted in an additional 57 segments being added. Since all segments were classified from the orthomosaic and not the underlying images, as it would considerably increase the manual labour, 9% of the segments were unidentifiable due to blurriness and distortion of the orthomosaic and 24.9% were annotated to the coarser classes 'other' ('_OTH'), including 9.7% *Pocillopora* (G_POC_OTH), 7.2% branching *Acropora* (AC_BRAN_OTH) and 5.3% massive coral (MAS_OTH).

2.10 | Model performance metrics

To evaluate RapidBenthos' performance, we used a two-step process to independently assess the capabilities of each AI tool, SAM

and ReefCloud. First, we examined the detection and segmentation accuracy of benthic components, and second, we assessed the classification accuracy. This is particularly important given that classification accuracy in ReefCloud depends on the model's training level, unlike SAM's unsupervised segmentation phase. Table 1 provides an overview of the experiments conducted to validate our method.

The first validation aimed at assessing the performance of RapidBenthos to segment benthic components from coral reef orthomosaics. As we are not performing any additional training to the published SAM model, it is likely that it has never been exposed to benthic imagery or underwater scenes. Therefore, verifying that the segments generated by this model align with ecologically relevant targets is essential. A pixel-wise comparison of the RapidBenthos output and validation data was performed. For reliable performance metrics, both datasets were filtered to include only the same benthic component classes, excluding background classes (i.e. sand, rubble, sponge and the algae sub-classes mostly composed of Turf). The filtered output and validation data were then converted to binary masks, where segmented regions were assigned 1 and the remaining pixel 0. These binary masks were enabled the evaluation of segmentation performance for benthic components in coral reef orthomosaics. Performance metrics used in the evaluation of this segmentation phase of the RapidBenthos workflow are described in the Appendix S5.

To quantify how accurately the predicted benthic components were segmented, IoU was calculated between the ground truth and predicted overlapping segments (Equation 2). The IoU is a measure of how well the predicted segment aligns with the actual object by quantifying the overlap between the predicted and the ground truth segments.

$$\text{IoU} = \frac{\text{Area of Overlap}}{\text{Area of Union}}. \quad (2)$$

Finally, a confusion matrix was used to evaluate the segment classification phase of the RapidBenthos workflow. The confusion matrix displays the distribution of model predictions for each class, highlighting which classes the model tends to 'confuse' with others. All these metrics range from zero to one. Scores closer to one indicate a higher level of agreement between model predictions and validation data, thereby reflecting a more accurate representation of the data.

3 | RESULTS

The RapidBenthos workflow automatically segmented and classified 2808 segments (Figure 3a) from 43 different classes, including 515 segments after filtering out background classes (Section 2.10) in one 40 sq. m orthomosaic. In comparison, the manual annotation of the same orthomosaic (Figure 3c) had 757 segments from 43 different classes, made up of 444 segments after filtering.

TABLE 1 Experiments conducted to validate the RapidBenthos workflow, along with their corresponding tests, evaluations and manuscript sections.

Experiment	Test	Evaluation	Section
RapidBenthos phase 1: Segmentation	Binary mask and IoU	SAM accuracy in delineating object	3.1 and Table 2
Point annotation model	F1 score	ReefCloud model classification accuracy	3.2, Figure 5 and Appendix S7
RapidBenthos phase 2: Classification	Confusion matrix	RapidBenthos accuracy in classifying object	3.2, Figure 6 and Appendix S7
Community composition	Per cent cover	RapidBenthos accuracy in extracting per cent cover	3.3 and Figure 7
Colony-level metrics	Colony count and planar area	RapidBenthos accuracy in extracting colony-level metrics	3.3 and Figure 7
RapidBenthos application to 11 diverse plots	IoU and classification of 'Acropora corymbose' colonies	RapidBenthos application across various coral reef environments	Supporting Information S1

TABLE 2 Validation metrics report between the validation and RapidBenthos overall segmentation, where zero represents the background pixels and one the pixels within segments.

	Precision	Recall	F1 score	Support
0	0.98	0.97	0.98	2,445,468,064
1	0.85	0.92	0.88	491,353,408
Accuracy			0.96	2,936,821,472
Macro avg.	0.92	0.94	0.93	2,936,821,472

3.1 | Performance of RapidBenthos segmentation phase

The overall accuracy of RapidBenthos segmentation phase was 0.96 (max. score of 1.0) indicating that it correctly identified 96% of the pixels either as background or benthic components (Table 1). The macro average F1 score was 0.93. The precision and recall for the benthic components were 0.85 and 0.92, respectively, resulting in a F1 score of 0.88. The confusion matrix for the background class and detected benthic constituent had a normalised score of 0.97 and 0.92, respectively (Appendix S6). This result implies that RapidBenthos correctly identified 97% of the background pixels as background (False–False), and 92% of the benthic constituent pixels were detected correctly (True–True). The overall IoU was 0.79 when comparing all segments but increased to 0.87 when selecting only overlapping segments. While the former IoU reflects SAM's object detection performance, the latter more accurately represents its segmentation precision. Calculating the IoU for overlapping segments indicates how closely SAM detected object edges compared with manual segmentation.

Upon visual inspection, the largest of the segmentation errors primarily resulted from distortion in the orthomosaic reconstruction causing errors on the edges of colonies (Figure 4). In these instances, the model either omitted (Figure 4a) or committed (Figure 4b) large section of segments, contributing to the observed discrepancies.

3.2 | Point classification model accuracy and performance of RapidBenthos classification phase

To assess the performance of the point classifier, 20% of the 33,937 manually annotated points were withheld from the classifier during training. Of the 73 classes included in the label set, 59 were present in the images collected off Lizard Island (Figure 1a) used in the ReefCloud model trained for the primary validation. The point classifier correctly identified 76% of the points in this test set, resulting in an overall F1 score of 0.821 (Figure 5). All the classes 'Other' (_OTH) were less accurate than their most specific counterparts, except for the coarse class 'Foliose'. This can be explained by training a class with points that are either from colonies similar to the ones included in the higher taxonomic resolution classes (e.g. *Acropora* Branching Other [ACO_Bran_OTH]) or that includes multiple disparate colonies (e.g. Massive Other [MAS_OTH]). The highest performing classes with a score of 1.0 were of uncommon and very distinct forms which included the classes 'Foliose Other Lettuce like' (FOL_OTH_L), 'Soft Coral Fan' (SCF), 'Soft Coral Whip' (SCW), 'Sponge Massive' (SPM) and 'Sponge Erect' (SPE).

When compared to the manual annotations, RapidBenthos' most accurate classification were 'Montipora' (G_MON), 'Star Fish' (MOB_SF), 'Acropora digitate' (ACD), 'Background', 'Acropora millepora' (ACO_MIL), 'Diploastrea' (G_DIP), 'Lobophyllia' (G_LOB) and 'Marker Dumbbell' (MDB), scoring above 0.96 in the confusion matrix (Figure 6). The least accurate high taxonomic resolution hard coral was 'Goniastrea' (G_GOS) with a score of 0.31. The confusion for this class was predominantly with 'Background'. This may be due to the small size of individuals (<8.51 cm²) found at this site, which were used in the ReefCloud training. As a result, some training patches contained a small proportion of pixels representing the targeted class, while the majority of pixels belonged to the 'Background' class (Appendix S10). Five classes had an accuracy of zero, with three of them belonging to the 'Other' category: 'Pocillopora Other' (G_POC_OTH), 'Coral Branching Other Coarse' (CB_OTH_C) and

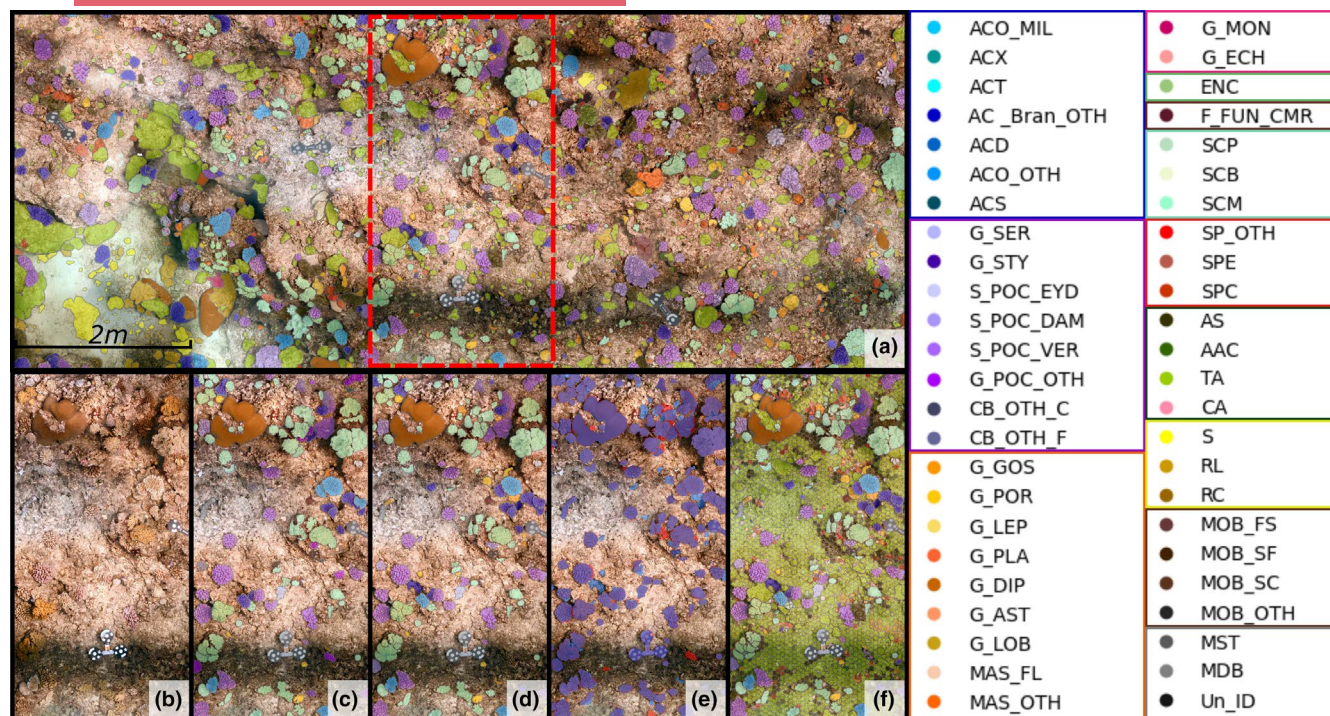


FIGURE 3 Figure showing the RapidBenthos output: (a) whole orthomosaic analysed; and a subset showing (b) unannotated orthomosaic; (c) validation (manually annotated) data; (d) RapidBenthos output filtered for performance metric assessment; (e) segmentation agreement between validation data (red) and RapidBenthos (blue) where overlapping segments are displayed in purple; and (f) community composition output. The legend represents all the benthic classes grouped by coarse-class hue where the 'Acropora' segments are blue, the 'branching non-Acropora' are purple, the 'massive' corals are orange, the 'foliose' corals are pink, the 'soft corals' are turquoise, the 'algae' are green, the 'mobile invertebrates' are brown, and the 'unidentifiable' black. The label set hierarchical design and meaning of the acronyms can be found in Appendix S2.

'Coral Branching Other Fine' (CB_OTH_F). Most pixels from these three classes were assigned to finer taxonomic classes, including '*Pocillopora verrucosa*' (S_POC_VER), '*Acropora* Branching Other' (ACO_Bran_OTH) and '*Pocillopora damicornis*' (S_POC_DAM), respectively. The class '*Leptoria*' (G_LEP) was confused with '*Platygyra*' (G_PLA), likely due to their similar appearance. Lastly, '*Acropora* Staghorn' was misclassified as '*Pocillopora verrucosa*' (S_POC_VER) due to a segmentation error. The majority of the detected pixels corresponding to the validation data 'unidentified' label were classified by the model as 'soft coral' (25%), '*Pocillopora verrucosa*' (S_POC_VER) (14%), '*Acropora* Branching Other' (ACO_Bran_OTH) (9%) and '*Porites*' (G_POR) (9%). This result suggests that RapidBenthos labelled segments that could not be identified manually from the orthomosaic.

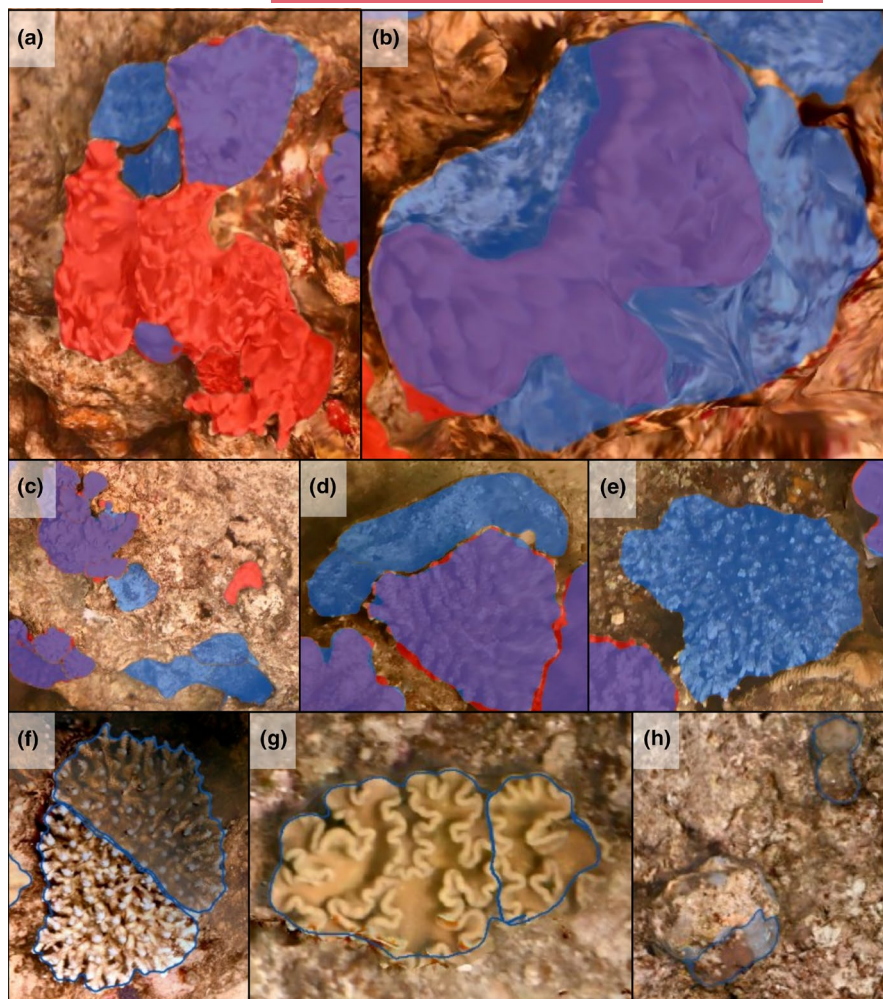
Annotation errors predominantly arose from obstructing features, often resulting from abrupt change in topography or the proximity of larger, overtopping benthic components (Figure 4c,d). Additionally, instances of commission errors were caused by the challenges in distinguishing between living and dead colonies, as dead colony was not a class trained in the annotation model (Figure 4e). The F1 score and confusion matrix per coarse class are displayed in Appendix S7.

3.3 | Community composition comparison

The predicted community composition in terms of per cent cover per class was closely related to the validation data (Figure 7a). For ease of reporting and visual clarity, we grouped the classes into eight categories. RapidBenthos slightly overestimated the per cent cover of most coarse class. The largest overestimate for coral colonies was 0.8% for the coarse class 'massive' coral. The biggest discrepancy was for the coarse class 'algae' which was underestimated by 6.4%. However, RapidBenthos detected 4% of 'encrusting sponge', which were not manually annotated. The prediction depicted the general trend for the number of colonies and colony size metrics (Figure 7b,c). The number of colonies was overestimated for most classes with the exception of 'Foliose', 'Fungiidae' and 'mobile biota', which had equal count to the validation data (Figure 7b). The coarse class 'massive' coral had the biggest colony count overestimate of 47 colonies. Conversely, the planar area was generally underestimated by the prediction (Figure 7c). The largest discrepancies were for the coarse classes 'massive' coral, 'foliose', 'mobile biota' and 'markers'.

The overestimation of colony count and the underestimation of planar area can be attributed to both the blurriness in model reconstruction, which leads to the generation of multiple segments

FIGURE 4 Example of segmentation errors where the validation segments are displayed in red, RapidBenthos segments in blue and overlapping segments in purple. (a) Error of omission shown by the red area and (b) error of commission shown by the blue area. Error of commission shown by the blue segments (c) caused by abrupt change in elevation, (d) obstruction by larger or overtopping benthic constituents and (e) misclassification of dead colonies. Example of coral colony automatically segmented by two segments due to (f) being half focused and half blurry, and (g) having complex shape. Both examples resulting in two smaller segments than the validation data. (h) Example of colonies detected by the model but omitted in the validation data.



per colony (Figure 4f), and the complex shapes of coral colonies (Figure 4g). Additionally, the model detected colonies that were omitted in the validation dataset (true negative), contributing to the higher colony count (Figure 4h).

4 | DISCUSSION

A significant challenge in leveraging large-area coral reef images lies in efficiently extracting metrics on benthic community composition, structure and function, such as diversity, abundance, location, size and how these change over time. We developed RapidBenthos, an automated workflow, to provide a fast, efficient and reliable process for accurately segmenting and classifying coral reef orthomosaics, thereby facilitating comprehensive data analyses and ecological assessment. In this study, we show that RapidBenthos was able to automatically detect 43 taxonomic benthic classes grouped into eight categories, with a segmentation accuracy of 0.96 and a F1 score of 0.88. These results highlight the strong potential of this method for automating the segmentation and classification of coral reef orthomosaics and to increase the number of classes and taxonomic resolution of previous automatic segmentation methods (Mizuno et al., 2020; Mohamed et al., 2022; Pavoni et al., 2021; Swanborn et al., 2022; Yuval et al., 2021).

Most notably, RapidBenthos demonstrated its efficiency in deriving community composition and colony-level metrics, achieving results in one-tenth of the time needed for manual segmentation and classification of the same orthomosaic (Section 2.9), and 195 times faster than human intervention efforts once the ReefCloud model is trained. This substantial reduction, from 65 h of manual labour to less than 6 h of computational time, requiring only 20 min of manual data handling, significantly alleviated the need for manual inputs. Such efficiency gains can enable unparalleled levels of information extraction compared with manual annotation methods for 2D reconstructions of coral reefs. This scalability allows for rapid assessments, long-term monitoring and fine-scale observations over massive extents, heralding a transformative shift in coral reef research and evidence-based environmental decision making.

The high IoU score (0.87) for segments created by RapidBenthos demonstrates the performance and accuracy of the SAM for detecting and segmenting benthic components in coral reef orthomosaics. The confusion matrix, comparing ReefCloud predictions with manual annotations, showed that most coarse classes scored within 0.04 of the corresponding F1 score of the point-based ReefCloud classification model, which indicates that the reported performance of the point classifier translated into accurate predictions on the mosaic pixels. This similarity between the training F1 score and the

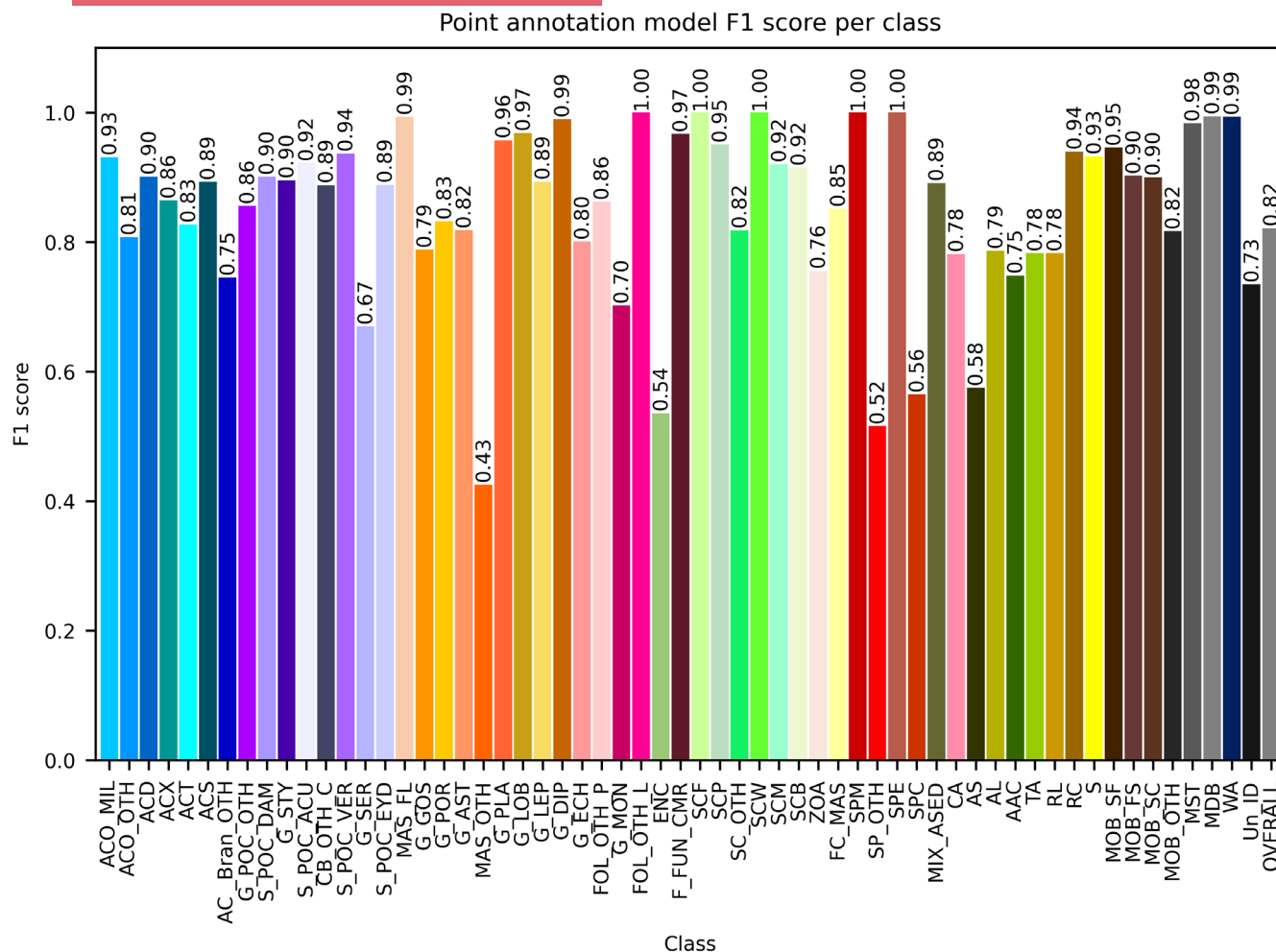


FIGURE 5 F1 score for all 59 classes present in the images used to train the ReefCloud point classification model for the primary validation site off Lizard Island.

classification validation highlights the significance of diligently training the point classification model.

Overall trends in community composition derived from RapidBenthos was representative of the validation data. RapidBenthos was able to quantify per cent cover of coral taxa at coarse taxonomic resolution within 0.8% of the validation data, showcasing the ability of the workflow to accurately quantify community composition from coral reef orthomosaics. As per the colony-level metrics, the overestimate in colony count and the underestimate in planar area can be explained by both the blurriness caused by orthorectification and the complex shapes of coral colonies (Li et al., 2024), leading to multiple segments per colony. For studies investigating coral demography, it is therefore recommended to conduct manual interventions (i.e. border refinement, merging/dividing segments and label correction) at the end of RapidBenthos workflow to increase the accuracy of the colony-level metrics. Moreover, manual refinement of colony borders is also essential for studies focused on coral growth. This is particularly crucial as coral growth measurements demand millimetre to centimetre resolution to accurately capture the slow growth rates of some corals (Ferrari et al., 2017; Razak et al., 2020).

Results of additional validation analyses of RapidBenthos at 11 sites across the GBR demonstrated that this method can be used in a range of environmental conditions, from clear offshore waters to turbid inshore reefs, at various depths (5–15 m), and for all reef habitats (i.e. reef front, flank, back and lagoon) (Supporting Information S1). Despite the wide range of coral reef environments and diverse benthic community assemblages (Figures S2 and S3), RapidBenthos was still able to achieve high accuracy in segmentation (IoU 0.92) (Table S1). Classification accuracy of RapidBenthos across these sites was also high, especially at the genus level of 'Acropora'. Overall, 88% of segments were assigned a class included in the 'Acropora' group, echoing the results of 0.89 from the 'Acropora' in the coarse-class confusion matrix of the primary validation plot (Appendix S7). However, further training would be beneficial to reduce the confusion between the *Acropora* *Corymbose* (ACO) and *Acropora* *Table* (ACT). Furthermore, all the colonies mislabelled by turf had generally a very small planar area ($<0.0025\text{m}^2$) indicating that the classification model might be less accurate for smaller segments. The classifier in ReefCloud's backend makes predictions based on an image patch centred on the point in question. If the target segment is smaller than this patch area, the model may misclassify the point

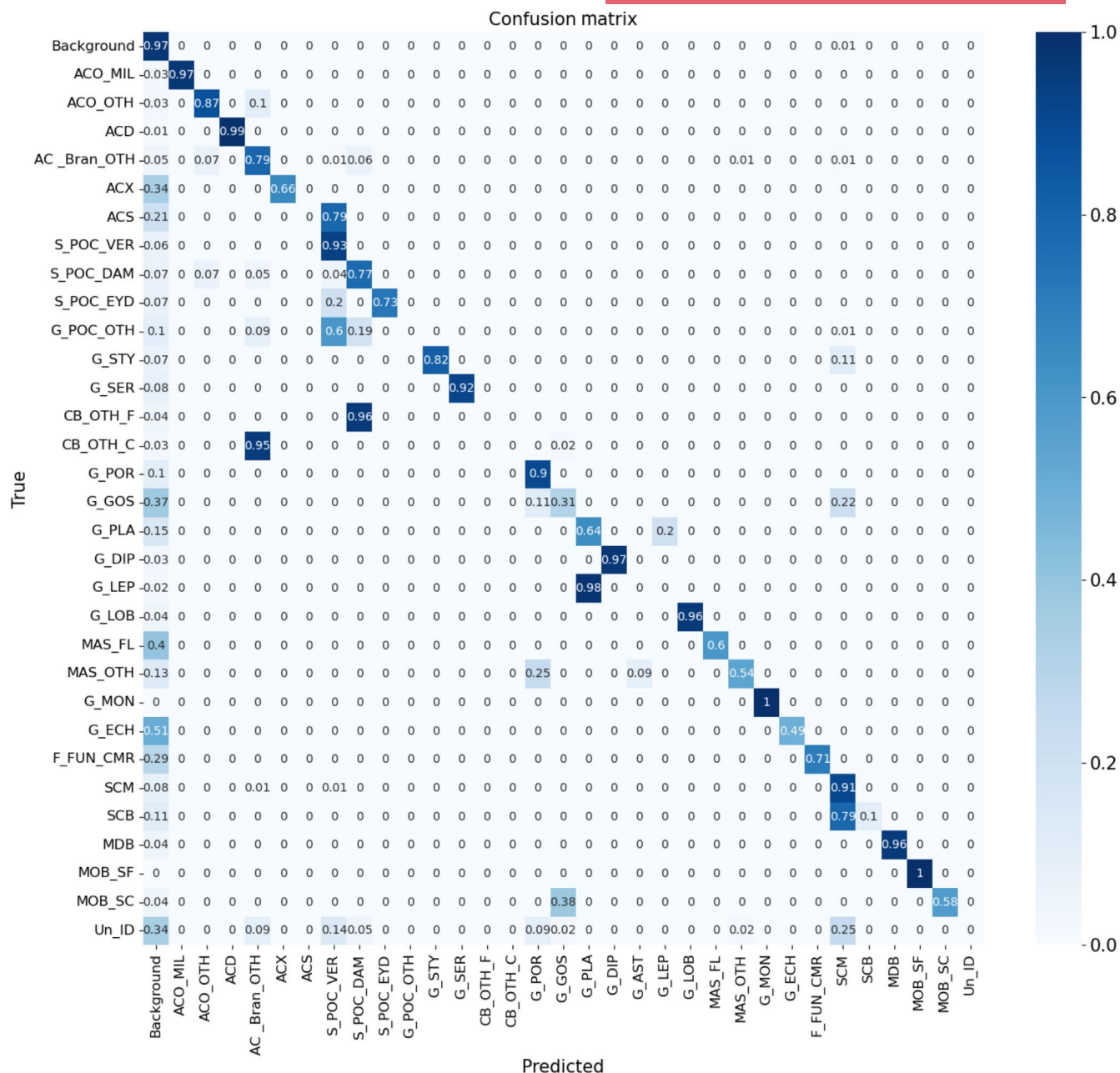


FIGURE 6 Confusion matrix for all 33 filtered classes between the validation data and RapidBenthos for performance metric assessment of the primary validation site off Lizard Island.

due to the presence of other classes in the patch (Appendix S8). This is why it is important to incorporate a minimum size threshold for segments based on the image patch size.

RapidBenthos offers key advantages over existing manual and semi-automated benthic segmentation techniques. Its integrated AI tools do not require retraining of deep neural networks (Kirillov et al., 2023), reducing computational demands and the need for ML expertise. This also eliminates the need for labour-intensive, fine-scale segmented training data. Developers aiming to train a deep learning model to segment coral reef orthomosaics can also utilise RapidBenthos to efficiently scale up the generation of training data for other applications. Moreover, the entire workflow is processed on Python IDE or HPC using a three-script chain, eliminating the

need for users to directly access Metashape. Due to RapidBenthos' capability to swiftly and automatically produce annotated segments, user input is limited to quality-checking and refining segment borders, significantly accelerating the segmentation process.

RapidBenthos leverages the best available data (the underlying images) to classify segments. Using the high-resolution images allows for classification with high taxonomic resolution. Consequently, the classification model is likely to achieve higher resolution and accuracy compared with a model trained directly on the orthomosaics. RapidBenthos also possesses functionality to incorporate custom classification models tailored to suit specific user needs. This is essential given the diversity of coral reef communities globally, the varied instruments with differing image resolutions used for coral reef

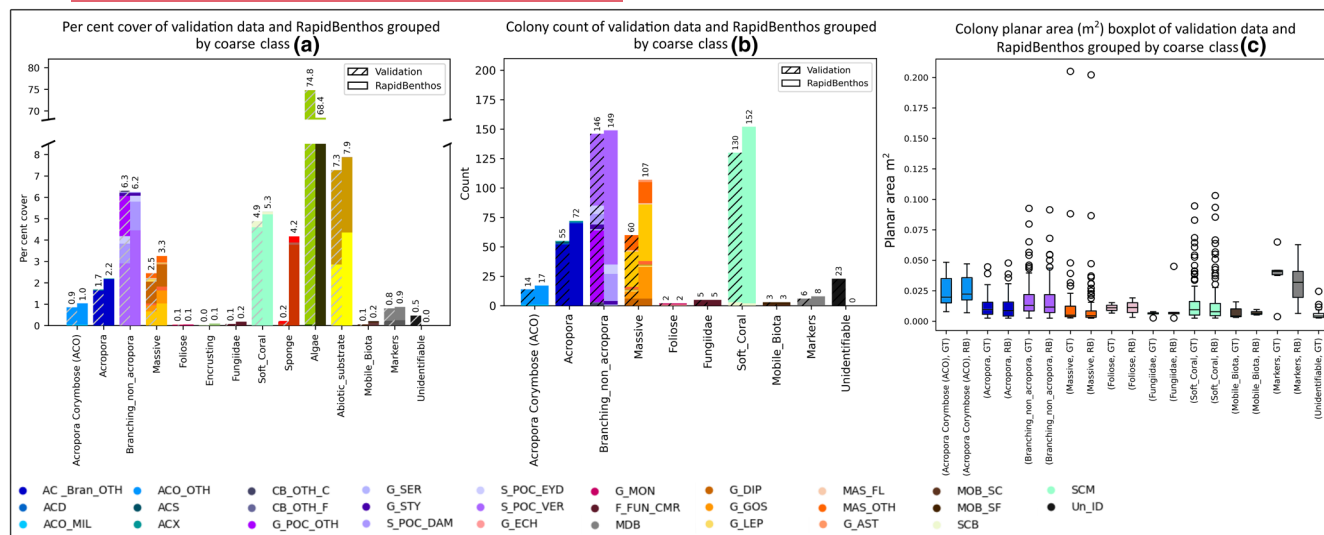


FIGURE 7 Performance of RapidBenthos against manually annotated validation data. (a) Per cent cover of taxa estimated by validation and RapidBenthos per class grouped by coarse classes; (b) number of colonies estimated by validation and RapidBenthos per class grouped by coarse classes, and; (c) boxplot of the estimated colonies planar area (in square metres) by validation (GT) and RapidBenthos (RB) per coarse class. The label set hierarchical design and meaning of the acronyms can be found in Appendix S2.

model reconstruction, and to capture targeted variables capable of answering specific research questions (González-Rivero et al., 2020; Remmers et al., 2023). This adaptability also supports the transition from photo-transect monitoring to photogrammetry, especially for research groups already utilising point classification tools like ReefCloud and CoralNet to quantify per cent coverage. The integration of pre-trained point classification models into RapidBenthos also enables the extraction of community composition data specific to the investigated site, further enhancing its applicability across a range of monitoring projects. Moreover, we have demonstrated that our model can be applied to one of the most complex environments, coral reefs and complex imagery sets, underwater photographs. Although we have only tested our model on orthomosaics of coral reefs, this workflow has strong potential to be applied to other complex environments surveyed using photogrammetry (e.g. forest canopies; Li et al., 2022, and urban areas; Iheaturu et al., 2022).

Although RapidBenthos presents numerous advantages, its main limitations stem from the high computing requirements and potential constraints on labelling accuracy due to imagery acquisition. Depending on the model size and image resolution, this method can demand high computing capacity. However, since building 3D coral reef reconstructions already requires access to substantial computational power, executing this workflow may not require additional hardware if such equipment is already available. Accordingly, while HPCs or powerful GPUs are not mandatory to execute the proposed workflow, incorporating them would considerably enhance processing speed.

Additional limitations affecting the accuracy of segmenting and labelling the orthomosaic are linked to the quality of underlying photographs and model reconstructions. Since coral reef 2D orthomosaics are a representation of real-life 3D environments, segmentation accuracy can be impacted by reconstruction quality

and characteristics of common natural objects. Factors such as blurriness, lack of contrasting colours and indistinct edges in photographs and orthomosaics may contribute to segmentation errors (Li et al., 2024), while label accuracy is influenced by complex topography, occlusions and the volume of training data for the point classifier. Furthermore, field data collection may impact class assignment accuracy. As shown in Figure 1c, the camera distribution had lower coverage in some plot sections, thereby resulting in segments being classified using more distant cameras and potentially increasing uncertainties in classification.

The images collected in this study followed a strict standard operational procedure (Gordon et al., 2023), which aimed at quantifying both 3D structural complexity and 2D benthic community composition (requiring both nadir and oblique imagery to be collected). When using RapidBenthos to quantify benthic community composition from 2D orthomosaics, image filtering to predominantly use nadir (top-down) image for orthomosaic production could help minimise segmentation and labelling errors. While RapidBenthos represents a significant step forward in the characterisation of marine benthic communities across large spatial extents, it only looks at a 2D representation of a 3D landscape. In the future, full automated segmentation and classification of large-area 3D terrain reconstructions will continue advancing ecological and evolutionary research (Pierce et al., 2021).

5 | CONCLUSIONS

In conclusion, RapidBenthos represents a major advance in coral reef research, addressing the critical challenge of rapidly extracting detailed benthic community and colony-level information from imagery. By using high-resolution images rather than orthomosaics for

classification, RapidBenthos achieves superior precision and accuracy, capturing of fine-scale features often lost in model reconstructions. This efficiency reduces the time and manual effort needed for segmentation, enabling rapid, large-scale monitoring of coral reefs with minimal user input. Its adaptability to various reef environments and the ability to integrate custom classification models further enhance its value for scientific research and conservation. Despite challenges in optimising imagery collection and processing speed, RapidBenthos—through its scalability, speed and accuracy—serves as a transformative tool for coral reef ecology, opening new avenues for addressing pressing environmental questions.

AUTHOR CONTRIBUTIONS

Tiny Remmers, Mathew Wyatt, Nader Boutros, Chirs Roelfsema and Renata Ferrari conceived the ideas; Tiny Remmers, Mathew Wyatt and Nader Boutros designed methodology; Tiny Remmers and Nader Boutros developed the software; Tiny Remmers, Sophie Gordon, Maren Toor and Marine Lechene participated to the data curation; Chirs Roelfsema, Katharina Fabricius, Alana Grech and Renata Ferrari supervised the research; Tiny Remmers conducted the validation, formal analysis, investigation, visualisation and writing of the original draft. All authors contributed critically to the drafts and gave final approval for publication.

ACKNOWLEDGEMENTS

This research was supported by the Reef Restoration and Adaptation Program funded by the partnership between the Australian Government's Reef Trust and the Great Barrier Reef Foundation, the Australian Institute of Marine Science, the College of Science and Engineering at James Cook University and the Remote Sensing Research Centre of the School of the Environment at the University of Queensland. The research was conducted under the Great Barrier Reef Marine Park permit G21/44774.1. We acknowledge the Wulgurukaba and Bindal people as the Traditional Owners of the land where this research was conducted. More broadly, we acknowledge the Traditional Owners of the Great Barrier Reef area and their continuing connection to their land and sea country. We would like to thank Mr. Benjamin Watkin for his information technology support throughout the development of the workflow.

CONFLICT OF INTEREST STATEMENT

The authors declare that they have no known competing financial interests or personal relationships that could have appeared to influence the work reported in this paper.

PEER REVIEW

The peer review history for this article is available at <https://www.webofscience.com/api/gateway/wos/peer-review/10.1111/2041-210X.14477>.

DATA AVAILABILITY STATEMENT

The data that support the findings of this study are archived in the Research Data JCU repository <https://doi.org/10.25903/hk08-qx50>

at James Cook University, Australia (Remmers et al., 2024a). The 3D models and underlying images' metadata are available in the Australian Institute of Marine Science <https://apps.aims.gov.au/metadata/view/5905b3eb-aad0-4f9c-a03e-a02fb3488082> (AIMS, 2024) and can be accessed on request. The RapidBenthos code is available on GitHub <https://github.com/tyremmers/RapidBenthos> and archived in Zenodo <https://doi.org/10.5281/zenodo.14219991> (Remmers et al., 2024b).

ORCID

Tiny Remmers  <https://orcid.org/0000-0002-0984-7940>

Mathew Wyatt  <https://orcid.org/0000-0003-2854-2664>

Alana Grech  <https://orcid.org/0000-0003-4117-3779>

REFERENCES

- Aber, J. S., Marzloff, I., & Ries, J. B. (2010). Chapter 3—Photogrammetry. In J. S. Aber, I. Marzloff, & J. B. Ries (Eds.), *Small-format aerial photography* (pp. 23–39). Elsevier. <https://doi.org/10.1016/B978-0-444-53260-2.10003-1>
- Althaus, F., Hill, N., Ferrari, R., Edwards, L., Przeslawski, R., Schönberg, C. H. L., Stuart-Smith, R., Barrett, N., Edgar, G., Colquhoun, J., Tran, M., Jordan, A., Rees, T., & Gowlett-Holmes, K. (2015). A standardised vocabulary for identifying benthic biota and substrata from underwater imagery: The CATAMI classification scheme. *PLoS One*, 10, 1–18. <https://doi.org/10.1371/journal.pone.0141039>
- Australian Institute of Marine Science (AIMS). (2024). RapidBenthos. <https://apps.aims.gov.au/metadata/view/5905b3eb-aad0-4f9c-a03e-a02fb3488082>
- Bayley, D. T. I., Mogg, A. O. M., Koldewey, H., & Purvis, A. (2019). Capturing complexity: Field-testing the use of "structure from motion" derived virtual models to replicate standard measures of reef physical structure. *PeerJ*, 2019, e6540. <https://doi.org/10.7717/peerj.6540>
- Beijbom, O., Edmunds, P. J., Kline, D. I., Mitchell, B. G., & Kriegman, D. (2012). Automated annotation of coral reef survey images. In *2012 IEEE conference on computer vision and pattern recognition* (pp. 1170–1177). IEEE.
- Bellwood, D. R., Pratchett, M. S., Morrison, T. H., Gurney, G. G., Hughes, T. P., Álvarez-Romero, J. G., Day, J. C., Grantham, R., Grech, A., Hoey, A. S., Jones, G. P., Pandolfi, J. M., Tebbett, S. B., Techera, E., Weeks, R., & Cumming, G. S. (2019). Coral reef conservation in the Anthropocene: Confronting spatial mismatches and prioritizing functions. *Biological Conservation*, 236, 604–615. <https://doi.org/10.1016/j.biocon.2019.05.056>
- Boström-Einarsson, L., Babcock, R. C., Bayraktarov, E., Ceccarelli, D., Cook, N., Ferse, S. C. A., Hancock, B., Harrison, P., Hein, M., Shaver, E., Smith, A., Suggett, D., Stewart-Sinclair, P. J., Vardi, T., & McLeod, I. M. (2020). Coral restoration—A systematic review of current methods, successes, failures and future directions. *PLoS One*, 15, e0226631. <https://doi.org/10.1371/journal.pone.0226631>
- Bowker, M. A., Rengifo-Faiffer, M. C., Antoninka, A. J., Grover, H. S., Coe, K. K., Fisher, K., Mishler, B. D., Oliver, M., & Stark, L. R. (2021). Community composition influences ecosystem resistance and production more than species richness or intraspecific diversity. *Oikos*, 130, 1399–1410. <https://doi.org/10.1111/oik.08473>
- Cordts, M., Omran, M., Ramos, S., Rehfeld, T., Enzweiler, M., Benenson, R., Franke, U., Roth, S., & Schiele, B. (2016). The cityscapes dataset for semantic urban scene understanding. In *2016 IEEE conference on computer vision and pattern recognition (CVPR)* (pp. 3213–3223). IEEE.
- Evans, M. C., Tulloch, A. I. T., Law, E. A., Raiter, K. G., Possingham, H. P., & Wilson, K. A. (2015). Clear consideration of costs, condition and

- conservation benefits yields better planning outcomes. *Biological Conservation*, 191, 716–727. <https://doi.org/10.1016/j.biocon.2015.08.023>
- Ferrari, R., Figueira, W. F., Pratchett, M. S., Boube, T., Adam, A., Kobelkowsky-Vidrio, T., Doo, S. S., Atwood, T. B., & Byrne, M. (2017). 3D photogrammetry quantifies growth and external erosion of individual coral colonies and skeletons. *Scientific Reports*, 7, 16737. <https://doi.org/10.1038/s41598-017-16408-z>
- Ferrari, R., Lachs, L., Pygas, D. R., Humanes, A., Sommer, B., Figueira, W. F., Edwards, A. J., Bythell, J. C., & Guest, J. R. (2021). Photogrammetry as a tool to improve ecosystem restoration. *Trends in Ecology & Evolution*, 36, 1093–1101. <https://doi.org/10.1016/j.tree.2021.07.004>
- Figueira, W., Ferrari, R., Weatherby, E., Porter, A., Hawes, S., & Byrne, M. (2015). Accuracy and precision of habitat structural complexity metrics derived from underwater photogrammetry. *Remote Sensing*, 7, 16883–16900. <https://doi.org/10.3390/rs71215859>
- González-Rivero, M., Beijbom, O., Rodríguez-Ramírez, A., Bryant, D. E. P., Ganase, A., Gonzalez-Marrero, Y., Herrera-Reveles, A., Kennedy, E. V., Kim, C. J. S., Lopez-Marciano, S., Markey, K., Neal, B. P., Osborne, K., Reyes-Nivia, C., Sampayo, E. M., Stolberg, K., Taylor, A., Vercelloni, J., Wyatt, M., & Hoegh-Guldberg, O. (2020). Monitoring of coral reefs using artificial intelligence: A feasible and cost-effective approach. *Remote Sensing*, 12, 489. <https://doi.org/10.3390/rs12030489>
- Gordon, S., Aston, E. A., Lechene, M., Harianto, J., Figueira, W., Gonzalez-Rivero, M., Bray, P., & Ferrari, R. (2023). *Standard operational procedure number 1: Overview and in-field workflow*. 62. <https://doi.org/10.25845/SE7T-PS86>
- Hamylton, S. M. (2017). Mapping coral reef environments: A review of historical methods, recent advances and future opportunities. *Progress in Physical Geography: Earth and Environment*, 41, 803–833. <https://doi.org/10.1177/0309133317744998>
- Hopkinson, B. M., King, A. C., Owen, D. P., Johnson-Roberson, M., Long, M. H., & Bhandarkar, S. M. (2020). Automated classification of three-dimensional reconstructions of coral reefs using convolutional neural networks. *PLoS One*, 15, 20. <https://doi.org/10.1371/journal.pone.0230671>
- Iheaturu, C., Okolie, C., Ayodele, E., Egogo-Stanley, A., Musa, S., & Ifejika Speranza, C. (2022). A simplified structure-from-motion photogrammetry approach for urban development analysis. *Remote Sensing Applications: Society and Environment*, 28, 100850. <https://doi.org/10.1016/j.rsase.2022.100850>
- Johnson-Roberson, M., Kumar, S., Pizarro, O., & Williams, S. (2006). Stereoscopic imaging for coral segmentation and classification. In *Proceedings of IEEE/MTS Oceans (OCEANS '06)* (pp. 1–6). IEEE. <https://doi.org/10.1109/OCEANS.2006.306876>
- Kirillov, A., Mintun, E., Ravi, N., Mao, H., Rolland, C., Gustafson, L., Xiao, T., Whitehead, S., Berg, A. C., Wan-Yen, L., Dollár, P., & Girshick, R. (2023). Segment anything. *arXiv*, arXiv:2304.02643. <https://doi.org/10.48550/arXiv.2304.02643>
- Kohler, K. E., & Gill, S. M. (2006). Coral point count with excel extensions (CPCe): A visual basic program for the determination of coral and substrate coverage using random point count methodology. *Computational Geosciences*, 32, 1259–1269. <https://doi.org/10.1016/j.cageo.2005.11.009>
- Lechene, M. A. A., Haberstroh, A. J., Byrne, M., Figueira, W., & Ferrari, R. (2019). Optimising sampling strategies in coral reefs using large-area mosaics. *Remote Sensing*, 11, 2907. <https://doi.org/10.3390/rs11242907>
- Li, L., Mu, X., Chianucci, F., Qi, J., Jiang, J., Zhou, J., Chen, L., Huang, H., Yan, G., & Liu, S. (2022). Ultrahigh-resolution boreal forest canopy mapping: Combining UAV imagery and photogrammetric point clouds in a deep-learning-based approach. *International Journal of Applied Earth Observation and Geoinformation*, 107, 102686. <https://doi.org/10.1016/j.jag.2022.102686>
- Li, M., Zhang, H., Gruen, A., & Li, D. (2024). A survey on underwater coral image segmentation based on deep learning. *Geo-spatial Information Science*, 1–25. <https://doi.org/10.1080/10095020.2024.2343323>
- Loke, L. H. L., & Chisholm, R. A. (2022). Measuring habitat complexity and spatial heterogeneity in ecology. *Ecology Letters*, 25, 2269–2288. <https://doi.org/10.1111/ele.14084>
- Luhmann, T. (2011). *Close range photogrammetry: Principles, techniques and applications*. Whittles Publishing.
- Madin, J. S., Hoogenboom, M. O., Connolly, S. R., Darling, E. S., Falster, D. S., Huang, D., Keith, S. A., Mizerek, T., Pandolfi, J. M., Putnam, H. M., & Baird, A. H. (2016). A trait-based approach to advance coral reef science. *Trends in Ecology & Evolution*, 31, 419–428. <https://doi.org/10.1016/j.tree.2016.02.012>
- Marre, G., Holon, F., Luque, S., Boissery, P., & Deter, J. (2019). Monitoring marine habitats with photogrammetry: A cost-effective, accurate, precise and high-resolution reconstruction method. *Frontiers in Marine Science*, 6, 15. <https://doi.org/10.3389/fmars.2019.00276>
- Miller, S., Yadav, S., & Madin, J. S. (2021). The contribution of corals to reef structural complexity in Kāne'ohe Bay. *Coral Reefs*, 40, 1679–1685. <https://doi.org/10.1007/s00338-021-02190-y>
- Mills, M. S., Ungermann, M., Rigot, G., den Haan, J., Leon, J. X., & Schils, T. (2023). Assessment of the utility of underwater hyperspectral imaging for surveying and monitoring coral reef ecosystems. *Scientific Reports*, 13, 21103. <https://doi.org/10.1038/s41598-023-48263-6>
- Mizuno, K., Terayama, K., Tabeta, S., Sakamoto, S., Matsumoto, Y., Sugimoto, Y., Ogawa, T., Sugimoto, K., Fukami, H., Sakagami, M., Deki, M., & Kawakubo, A. (2020). Development of an efficient coral-coverage estimation method using a towed optical camera Array system [speedy sea scanner (SSS)] and deep-learning-based segmentation: A sea trial at the Kujuku-Shima Islands. *IEEE Journal of Oceanic Engineering*, 45, 1386–1395. <https://doi.org/10.1109/JOE.2019.2938717>
- Mohamed, H., Nadaoka, K., & Nakamura, T. (2022). Automatic semantic segmentation of benthic habitats using images from towed underwater camera in a complex shallow water environment. *Remote Sensing*, 14, 1818. <https://doi.org/10.3390/rs14081818>
- Nocerino, E., Menna, F., Gruen, A., Troyer, M., Capra, A., Castagnetti, C., Rossi, P., Brooks, A. J., Schmitt, R. J., & Holbrook, S. J. (2020). Coral reef monitoring by scuba divers using underwater photogrammetry and geodetic surveying. *Remote Sensing*, 12, 3036. <https://doi.org/10.3390/RS12183036>
- Nolan, M. K. B., Kim, C. J. S., Hoegh-Guldberg, O., & Beger, M. (2021). The benefits of heterogeneity in spatial prioritisation within coral reef environments. *Biological Conservation*, 258, 8. <https://doi.org/10.1016/j.biocon.2021.109155>
- Obura, D. O., Aeby, G., Amorntthammarong, N., Appeltans, W., Bax, N., Bishop, J., Brainard, R. E., Chan, S., Fletcher, P., Gordon, T. A. C., Gramer, L., Gudka, M., Halas, J., Hendee, J., Hodgson, G., Huang, D., Jankulak, M., Jones, A., Kimura, T., ... Wongbusarakum, S. (2019). Coral reef monitoring, reef assessment technologies, and ecosystem-based management. *Frontiers in Marine Science*, 6, 21. <https://doi.org/10.3389/fmars.2019.00580>
- Pavoni, G., Corsini, M., Callieri, M., Fiameni, G., Edwards, C., & Cignoni, P. (2020). On improving the training of models for the semantic segmentation of benthic communities from orthographic imagery. *Remote Sensing*, 12, 3106. <https://doi.org/10.3390/RS12183106>
- Pavoni, G., Corsini, M., Ponchio, F., Muntoni, A., Edwards, C., Pedersen, N., Sandin, S., & Cignoni, P. (2021). TagLab: AI-assisted annotation for the fast and accurate semantic segmentation of coral reef orthoimages. *Journal of Field Robotics*, 39, 246–262. <https://doi.org/10.1002/rob.22049>
- Pierce, J., Butler, M. J., Rzhano, Y., Lowell, K., & Dijkstra, J. A. (2021). Classifying 3-D models of coral reefs using structure-from-motion and multi-view semantic segmentation. *Frontiers in Marine Science*, 8. <https://doi.org/10.3389/fmars.2021.706674>

- Razak, T. B., Roff, G., Lough, J. M., & Mumby, P. J. (2020). Growth responses of branching versus massive corals to ocean warming on the Great Barrier Reef, Australia. *Science of the Total Environment*, 705, 135908. <https://doi.org/10.1016/j.scitotenv.2019.135908>
- ReefCloud. (2022). ReefCloud [WWW document]. ReefCloud. <https://reefcloud.ai/>
- Remmers, T., Boutros, N., & Wyatt, M. (2024a). Data from: RapidBenthos: Automated segmentation and multi-view classification of coral reef communities from photogrammetric reconstruction. *James Cook University*, <https://doi.org/10.25903/hk08-qx50>
- Remmers, T., Boutros, N., & Wyatt, M. (2024b). Code from: RapidBenthos: Automated segmentation and multi-view classification of coral reef communities from photogrammetric reconstruction. *Zenodo*, <https://doi.org/10.5281/zenodo.14219991>
- Remmers, T., Grech, A., Roelfsema, C., Gordon, S., Lechene, M., & Ferrari, R. (2023). Close-range underwater photogrammetry for coral reef ecology: A systematic literature review. *Coral Reefs*, 43, 35–52. <https://doi.org/10.1007/s00338-023-02445-w>
- Rossi, P., Ponti, M., Righi, S., Castagnetti, C., Simonini, R., Mancini, F., Agraftiotis, P., Bassani, L., Bruno, F., Cerrano, C., Cignoni, P., Corsini, M., Drap, P., Dubbini, M., Garrabou, J., Gori, A., Gracias, N., Ledoux, J. B., Linares, C., ... Capra, A. (2021). Needs and gaps in optical underwater technologies and methods for the investigation of marine animal Forest 3D-structural complexity. *Frontiers in Marine Science*, 8. <https://doi.org/10.3389/fmars.2021.591292>
- Schürholz, D., & Chennu, A. (2022). Digitizing the coral reef: Machine learning of underwater spectral images enables dense taxonomic mapping of benthic habitats. *Methods in Ecology and Evolution*, 14, 596–613.
- Shihavuddin, A. S. M., Grácias, N. R. E., García Campos, R., Gleason, A. C. R., & Gintert, B. (2013). Image-based coral reef classification and thematic mapping. *Remote Sensing*, 5, 1809–1841.
- Swanborn, D. J. B., Stefanoudis, P. V., Huvenne, V. A. I., Pittman, S. J., & Woodall, L. C. (2022). Structure-from-motion photogrammetry demonstrates that fine-scale seascape heterogeneity is essential in shaping mesophotic fish assemblages. *Remote Sensing in Ecology and Conservation*, 8, 904–920. <https://doi.org/10.1002/rse2.290>
- Urbina-Barreto, I., Chiroleu, F., Pinel, R., Frechon, L., Mahamadaly, V., Elise, S., Kulbicki, M., Quod, J. P., Dutrieux, E., Garnier, R., Bruggemann, J. H., Penin, L., & Adjeroud, M. (2021). Quantifying the shelter capacity of coral reefs using photogrammetric 3D modeling: From colonies to reefscales. *Ecological Indicators*, 121, 12. <https://doi.org/10.1016/j.ecolind.2020.107151>
- Urbina-Barreto, I., Garnier, R., Elise, S., Pinel, R., Dumas, P., Mahamadaly, V., Facon, M., Bureau, S., Peignon, C., Quod, J. P., Dutrieux, E., Penin, L., & Adjeroud, M. (2021). Which method for which purpose? A comparison of line intercept transect and underwater photogrammetry methods for coral reef surveys. *Frontiers in Marine Science*, 8, 636902. <https://doi.org/10.3389/fmars.2021.636902>
- Vercelloni, J., Roelfsema, C., Kovacs, E. M., González-Rivero, M., Moores, M. T., Logan, M., & Mengersen, K. (2024). Fine-scale interplay between decline and growth determines the spatial recovery of coral communities within a reef. *Ecography*, 2024, e06818. <https://doi.org/10.1111/ecog.06818>
- Wu, Q., & Osco, L. P. (2023). Samgeo: A python package for segmenting geospatial data with the segment anything model (SAM). *Journal of Open Source Software*, 8, 5663.
- Yuval, M., Alonso, I., Eyal, G., Tchernov, D., Loya, Y., Murillo, A. C., & Treibitz, T. (2021). Repeatable semantic reef-mapping through photogrammetry and label-augmentation. *Remote Sensing*, 13, 1–19. <https://doi.org/10.3390/rs13040659>

SUPPORTING INFORMATION

Additional supporting information can be found online in the Supporting Information section at the end of this article.

Data S1: RapidBenthos additional validation.

Data S2: Appendices.

How to cite this article: Remmers, T., Boutros, N., Wyatt, M., Gordon, S., Toor, M., Roelfsema, C., Fabricius, K., Grech, A., Lechene, M., & Ferrari, R. (2025). RapidBenthos: Automated segmentation and multi-view classification of coral reef communities from photogrammetric reconstruction. *Methods in Ecology and Evolution*, 16, 427–441. <https://doi.org/10.1111/2041-210X.14477>